Pores Formed by Single Subunits in Mixed Dimers of Different CLC Chloride Channels*

Frank Weinreich and Thomas J. Jentsch‡

From the Zentrum für Molekulare Neurobiologie Hamburg, ZMNH, Hamburg University, Martinistrasse 85, D-20246 Hamburg, Germany

CLC chloride channels comprise a gene family with nine mammalian members. Probably all CLC channels form homodimers, and some CLC proteins may also associate to heterodimers. ClC-0 and ClC-1, the only CLC channels investigated at the single-channel level, display two conductances of equal size which are thought to result from two separate pores, formed individually by the two monomers. We generated concatemeric channels containing one subunit of ClC-0 together with one subunit of ClC-1 or ClC-2. They should display two different conductances if one monomer were sufficient to form one pore. Indeed, we found a 8-picosiemens (pS) conductance (corresponding to ClC-0) that was associated with either a 1.8-pS (ClC-1) or a 2.8-pS (ClC-2) conductance. These conductances retained their typical gating, but the slow gating of ClC-0 that affects both pores simultaneously was lost. ClC-2 and ClC-0 current components were modified by point mutations in the corresponding subunit. The ClC-2 single pore of the mixed dimer was compared with the pores in the ClC-2 homodimer and found to be unaltered. We conclude that each monomer individually forms a gated pore. CLC dimers in general must be imagined as having two pores, as shown previously for ClC-0.

The pore architecture of anion channels is still poorly known. Structure-function studies have been undertaken for a number of structurally unrelated chloride channel classes, such as cystic fibrosis transmembrane conductance regulator (1, 2), ligand-gated anion channels (3), and CLC channels (4). Sedimentation studies suggested that ClC-0 (5), ClC-1 (6), and a bacterial CLC protein (7) are dimers. For the bacterial CLC, this was confirmed by cross-linking experiments. In single-channel recordings, ClC-0 displays two conductance levels of equal magnitude. These gate independently, but are shut off together by a different, slow gating process. This led to the suggestion that ClC-0 is a "double-barreled" channel, which has two identical, largely independent pores (8). This model was confirmed by studies in which only of the subunits in the homodimer was mutated (9, 10). These channels displayed single-channel conductances that were compatible with one wild-type pore and one mutated pore. The important question if each subunit individually forms a pore has also been addressed for ClC-0. Concatemers with two mutant

subunits suggested that one subunit forms one pore (10), although the presence of two mixed pores, formed by different parts of each subunit, could not be completely ruled out. However, the double-barreled structure of CLC channels has recently been questioned. The effect on whole cell-currents caused by the modification of cysteines in mutant ClC-1 channels led to the suggestion (11) that the two subunits of ClC-1 form a single pore that includes the D3-D4 region from each subunit. In single-channel records, however, ClC-1 displays a double-pore behavior comparable to that of ClC-0 (12). All CLC channels identified so far are homologous in the entire segment encompassing the 10–12 transmembrane domains. Hence, a common pore architecture must be assumed. This implies that either the "one-subunit/one-pore" model postulated for ClC-0 is valid for all members of this gene family, or it is valid for none of the channels, including ClC-0.

To demonstrate the functional and structural separation of individual pores in a CLC channel dimer, we constructed concatemers of two CLC channel monomers, linked in a head-to-tail fashion. The expression of concatenated subunits rather than coexpression of the corresponding monomers offers the advantage that only a single type of dimer will be formed. This approach has been used in the past to demonstrate separate pores in the ClC-0 channel (9, 10, 13). We now extend it to the study of concatemers composed of different CLC monomers, namely those of ClC-0, -1, and -2. Both ClC-1 and ClC-2 are highly homologous to ClC-0, with 54% and 49% identity at the amino acid level, respectively (14, 15). ClC-1 and ClC-2, which share 55% of sequence identity (15), have already been shown to form functional mixed dimers with altered properties in coexpression experiments (16).

Since ClC-0 has been studied extensively on the single-channel level (8, 13, 17, 18), its presence in the mixed channels may be demonstrated unambiguously by single-channel analysis. Only one study (12) showed single-channel recordings of ClC-1, and single ClC-2 channels have not yet been reported. In mixed concatemers of ClC-0, -1, and -2, we observed properties of both constituent pores in the macroscopic current. In single-channel recordings, we could clearly distinguish two different conductance levels that can be attributed to the pores of the constituent subunits. This demonstrates that one CLC subunit forms one pore, which retains most of its properties in a dimer irrespective of its partner. This is also the first time that single-channel traces of the ClC-2 pore are reported.

EXPERIMENTAL PROCEDURES

Construction of Concatemeric Channels and Expression in Xenopus Oocytes—To generate concatemeric channels, the stop codon of the N-terminal subunit was replaced with a *Pac*I restriction site, which was then used to link it to the C-terminal subunit. The linker sequence consisted of four amino acids (L-I-K-A). Point mutations were intro-
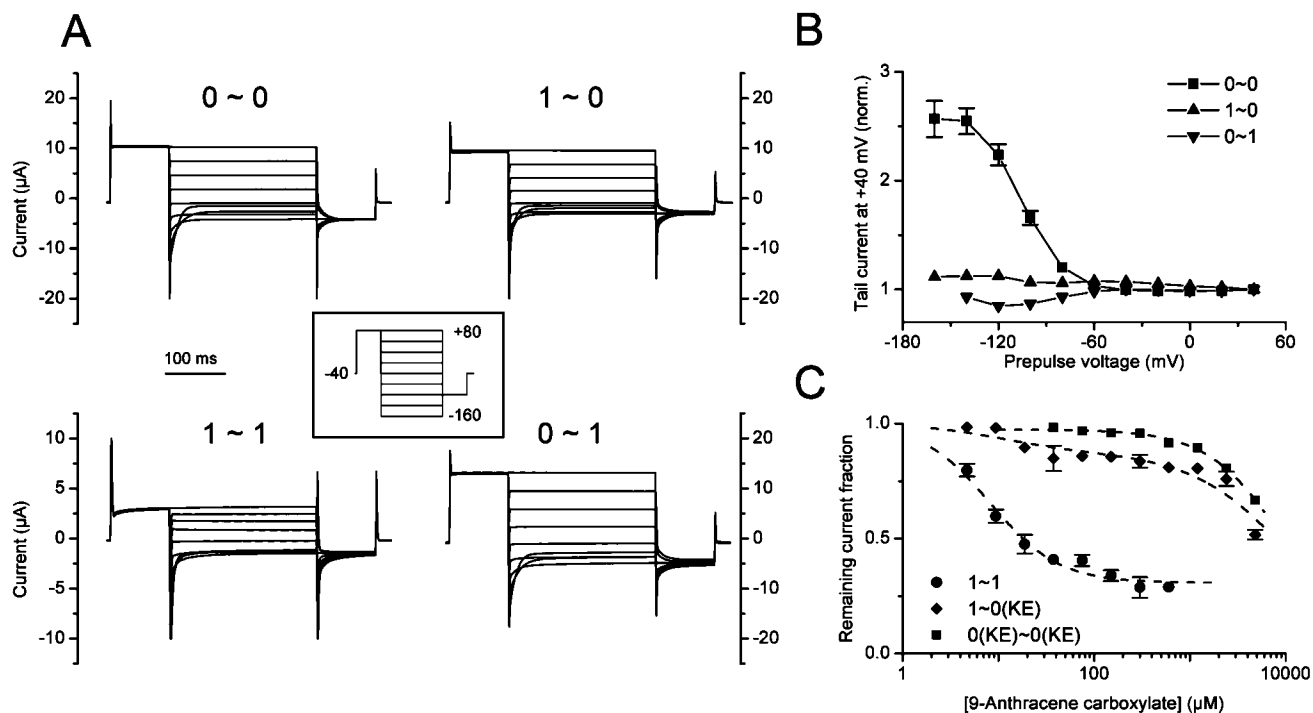
FIG. 1. **Macroscopic properties of mixed concatemers of ClC-0 and ClC-1.** *A*, families of current traces, obtained with the voltage protocol depicted in the insert, are shown for the four possible combinations of concatemers consisting of ClC-0 and/or ClC-1. The ClC-1 concatemer clearly exhibits the properties of ClC-1, yet the two mixed concatemers are indistinguishable from the ClC-0 concatemer. *B*, the ratio of the tail current at +40 mV, obtained after a 7-s prepulse to the indicated potential, to the current obtained with a +40-mV prepulse is a measure of the hyperpolarization-activated slow common gate of ClC-0 (29). When this is compared for the different concatemers, the ClC-0 concatemer shows a considerable activation starting at ~-60 mV, whereas both mixed concatemers lack this activation by hyperpolarization. *C*, the sensitivity to the inhibitor 9-AC is shown for three concatemers consisting of ClC-1 and/or ClC-0(K519E) subunits, which have almost equal single-channel conductances. The ClC-0(K519E) concatemer has an apparent IC_{50} of 9.8 ± 0.1 mM, the ClC-1 concatemer of 8.2 ± 1.0 μM. In the mixed concatemer, a small fraction of the current (about 12%) is inhibitable by small concentrations of 9-AC ($IC_{50} = 10.6 \pm 11.7$ μM) and the remainder is inhibited by much higher concentrations ($IC_{50} = 10.7 \pm 3.4$ mM). Note that the 9-AC dependence of the 1~0 current, in contrast to those of the homodimeric concatemers, is not well fitted by the function used to determine the IC_{50}. Data points in *B* and *C* represent the mean ± S.E. of three to six individual determinations. *Error bars* smaller than the symbol size are not shown.

duced by recombinant PCR[1] and verified by sequencing. Constructs were expressed in the pTLN vector (16), and capped cRNA was transcribed *in vitro* with the mMessage mMachine kit (Ambion, Austin, TX). 8–10 ng of cRNA were injected into *Xenopus* oocytes as described (19), and measurements were performed 2–4 days after injection, with mock-injected oocytes as controls.

Electrophysiology—Voltage-clamp measurements were performed using a conventional two-electrode voltage clamp (Turbo Tec 01C, npi, Tamm, Germany) in ND96 solution (96 mM NaCl, 2 mM KCl, 1.8 mM CaCl$_2$, 1 mM MgCl$_2$, 5 mM HEPES, pH 7.4). For inhibitor measurements, oocytes were continuously superfused with ND96 containing varying concentrations of 9-AC, up to the solubility limit, which was ~4 mM at neutral pH. Voltage protocols were generated using pClamp software (Axon Instruments, Foster City, CA). Patch clamp measurements were performed in the excised inside-out mode after manual removal of the vitellin envelope. Patch pipettes of 2–3-megohm resistance were made from aluminosilicate glass (Hilgenberg, Malsfeld, Germany), coated with Sylgard (General Electric, Waterford, NY), and filled with 100 mM NMG-Cl, 5 mM MgCl$_2$, 5 mM HEPES, pH 7.4. The bath solution contained 106 mM NMG-Cl, 2 mM MgCl$_2$, 2.5 mM EGTA, 5 mM HEPES, pH 7.4, resulting in a symmetrical chloride concentration of 110 mM. Data were acquired with an Axopatch 200B amplifier (Axon Instruments) using pClamp software, low pass-filtered at 1 or 4 kHz, and recorded on digital tape or on a hard disc, with acquisition rates of 2 and 10 kHz, respectively. For display purposes, single-channel data were digitally filtered at 330 Hz.

Data Analysis—To determine the IC_{50} values for 9-AC (Fig. 1*C*), the following function was used.

$$I/I_0 = (1 - I_{min})/(1 + (c/IC_{50})^n) + I_{min} \qquad \text{(Eq. 1)}$$

c denotes the inhibitor concentration and I_{min} the current remaining at

saturating inhibitor concentration. For the mixed concatemer with two inhibitor binding sites, the following function was fitted to the data.

$$I/I_0 = (1 - I_1)/(1 + (c/IC_{50/1})^{n1}) + (I_1 - I_{min})/(1 + (c/IC_{50/2})^{n2}) + I_{min} \qquad \text{(Eq. 2)}$$

I_1 is the current remaining at saturating inhibitor concentration for the high affinity binding site and I_{min} the current remaining at saturating concentration for the low affinity binding site.

Single-channel current amplitudes were calculated from Gaussian fits to all-points histograms. Mean open times were obtained from exponential fits to dwell-time histograms. Fitting was done using the Origin analysis software (Microcal Software, Northampton, MA).

RESULTS

Mixed Concatemers of ClC-1 and ClC-0—To test whether different CLC subunits may associate to form mixed pores with novel characteristics, or whether one pore is formed exclusively by one subunit, we constructed mixed concatemers of two CLC monomers. For simplicity, we will describe our results in the framework of the one-subunit/one-pore model and evaluate alternative models in the discussion section.

Using a four-amino acid linker sequence (see "Experimental Procedures"), ClC-0 and ClC-1 were linked in both possible orientations, *i.e.* ClC-1~ClC-0 and ClC-0~ClC-1. For comparison, homomeric concatemers of ClC-1 and of ClC-0 with the same linker sequence were constructed. All four concatemers could be expressed functionally in *Xenopus* oocytes (Fig. 1*A*). Apart from a reduced expression efficiency, no conspicuous differences were found between concatemeric and monomeric ClC-0, in accordance with previous studies of concatenated ClC-0 (10, 13), which reported wild-type behavior for macroscopic and single-channel properties of the concatemer. This

---

[1] The abbreviations used are: PCR, polymerase chain reaction; NMG, *N*-methyl-D-glucamine; 9-AC, 9-anthracene carboxylate; S, siemens.

indicated that concatemerization *per se* did not alter channel properties.

The current amplitudes for the different concatemers differed significantly at the peak of expression (3 days after RNA injection). The slope conductance at 0 mV of the 0~0 concatemer (116 ± 23 μS) was about 4–5 times higher than for the 1~1 concatemer (26 ± 6 μS), and the two mixed concatemers had conductances of 67 ± 21 μS in the 1~0 and 159 ± 24 μS in the 0~1 orientation (n = 10–21). Protein levels were not measured, so the differences in steady-state current amplitudes may be caused either by a different conductance or by differences in expression level. In general, however, current amplitudes increased with the number of ClC-0 subunits in the concatemer, consistent with the higher single-channel conductance of ClC-0 (8 pS (Ref. 19)) as compared with ClC-1 (1.2 pS (Ref. 12)).

Both ClC-0 and ClC-1 are voltage-gated in more than one way. This has been described as a "fast" gate and a "slow" gate for ClC-0 (8, 18). Although the slow gate in ClC-1 is much faster than in ClC-0, the same terminology has been used for ClC-1 by Pusch and co-workers (12). The voltage dependence of the fast gate is qualitatively similar for ClC-0 and ClC-1. Both channels are closed by hyperpolarization, with the midpoint of the activation curve at −100 mV for ClC-0 (20) and −20 mV for ClC-1 (21) in the oocyte system. Normal gating of ClC-1 is retained in the ClC-1~ClC-1 concatemer. However, no ClC-1-like currents were seen in the mixed concatemers with ClC-0. When a fast voltage protocol was used, their currents were very similar to ClC-0 (Fig. 1*A*). The steady-state current voltage dependence of the 1~0 and 0~1 concatemers was indistinguishable from that of the 0~0 concatemer (data not shown). Because of its lower single-channel conductance, the contribution of ClC-1 to the macroscopic current is expected to be small in mixed concatemers with ClC-0 (∼10%), but it should still be detectable. Although indistinguishable in their fast gating, both mixed concatemers differ from the ClC-0 concatemer by the absence of the hyperpolarization-activated slow gate, indicating that a different channel than in the 0~0 concatemer is formed (Fig. 1*B*).

The conclusion that the ClC-1 pore does not contribute significantly to macroscopic currents of the mixed concatemers is further supported by currents obtained from concatemers bearing the K519E mutation in the ClC-0 pore. Although the single-channel conductances of ClC-1 (1.2 pS (Ref. 12)) and ClC-0(K519E) (1 pS (Ref. 10)) are about equal, the macroscopic current of the mixed concatemers was very similar to the current obtained with the ClC-0(K519E) homodimer in terms of steady-state voltage dependence and open channel rectification. This was true irrespective of the order of the two subunits in the mixed concatemer (data not shown). However, the differential sensitivity of ClC-1 and ClC-0 to the inhibitor 9-AC (14, 22) may be exploited to demonstrate the presence of a ClC-1 conductance in the 1~0(K519E) concatemer. Extracellular 9-AC inhibited the ClC-1 concatemer with an apparent IC$_{50}$ of 8.2 ± 1.0 μM (Fig. 1*C*). This inhibition was not complete, because about 30% of the current remained at 500 μM 9-AC. The ClC-0(K519E) concatemer could only be inhibited by much higher 9-AC concentration, with an apparent IC$_{50}$ of 9.8 ± 0.8 mM. In the mixed concatemer, a biphasic inhibition was observed. A small fraction of the current (about 12%) was inhibited by similar concentrations of 9-AC as was the ClC-1 (IC$_{50}$ of 10.6 ± 11.7 μM), whereas the remaining current required equally high 9-AC concentrations as the ClC-0(K519E) to become blocked (IC$_{50}$ of 10.7 ± 3.4 mM). This indicates that the macroscopic current of the 1~0(K519E) concatemer is the sum of two current components with the same 9-AC sensitivity as the ClC-1 and ClC-0(K519E), respectively. Contrary to expec-
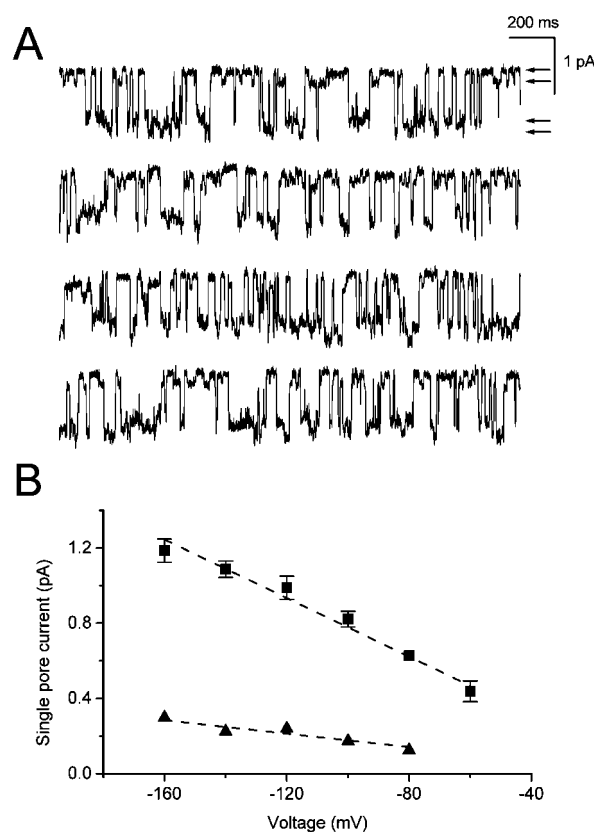

FIG. 2. **Single-channel properties of the ClC-1~ClC-0 mixed concatemer.** *A*, a continuous current trace of a single channel of the 1~0 concatemer, recorded at −100 mV, is shown. Four current levels (*arrows*) resulting from the presence of two different pores can be distinguished. The gating of both pores is independent of each other, because all possible gating transitions are observed between the four levels with equal likelihood, regardless of whether the other pore is open or closed (see "Results"). *B*, the single-pore conductance is determined from the current-voltage relationship in the range −80 to −160 mV. The conductance of the small pore (*triangles*) is 1.8 ± 0.1 pS; that of the large pore (*squares*) is 7.8 ± 0.2 pS, calculated from a linear fit to the data. Data points represent the mean ± S.E. of 3–12 individual determinations.

tation, the highly 9-AC-sensitive component is much smaller in amplitude than the 9-AC-insensitive component. This indicates that the activity of ClC-1 is reduced in the concatemer.

Since the properties of single ClC-0 and ClC-1 pores are known, it should be evident from single-channel currents of the mixed concatemer if both pores are present. Excised patches of 1~0 concatemers clearly showed two different pores, a large pore with the typical properties of a single ClC-0 pore and a small pore with properties of a ClC-1 pore (Fig. 2*A*). These two pores were invariably found together in the patch (12 out of 12 patches). The single-pore current voltage relationship was linear in the range of −60 and −160 mV (−80 and −160 mV for the small pore). Mean conductance of the small pore was 1.8 pS, about 50% larger than reported for wild-type ClC-1 pore at a lower pH of 6.5 (12). The conductance of the large pore was 7.8 pS and thus of the same magnitude as in the ClC-0 homodimer (∼8 pS) (Ref. 13 and data not shown).

Dwell-time analysis was performed in three patches with a stable single-channel at −100 mV. The large pore had a mean open time of 34 ± 2 ms, which is in the range reported for individual pores in the ClC-0 dimer (17, 18). The small pore had a mean open time of 29 ± 2 ms, slightly shorter than that of individual pores in the ClC-1 dimer at pH 6.5 (∼45 ms at −140 mV (Ref. 12)). This difference is expected because a lower pH slows the overall gating of ClC-1 (23). Very long closed times
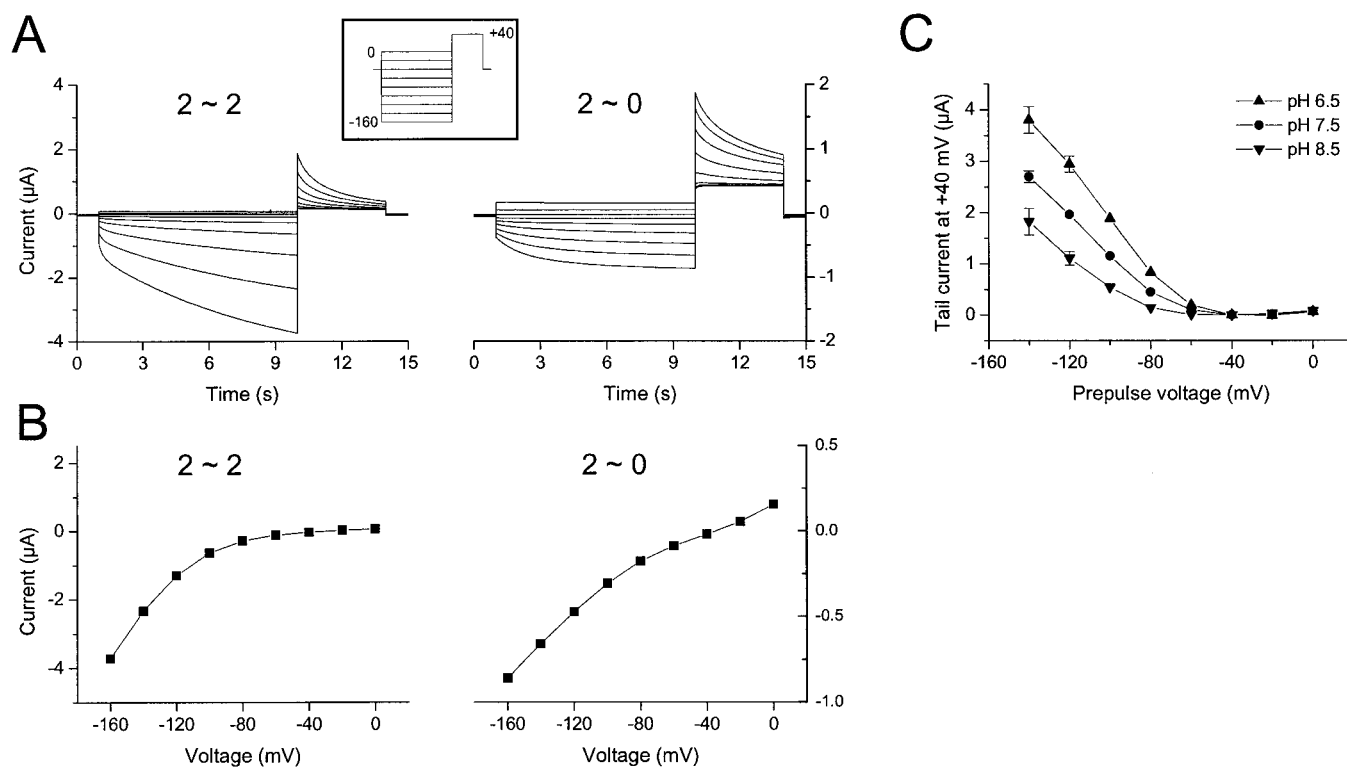
FIG. 3. **Macroscopic properties of mixed concatemers of ClC-0 and ClC-2.** *A*, families of current traces, obtained with the voltage protocol depicted in the insert, are shown for the 2~2 and 2~0 concatemers. *B*, steady-state current-voltage relationships for the traces shown in *A*. The 2~2 concatemer yields only hyperpolarization-activated currents, the 2~0 concatemer can be activated both by depolarization and by hyperpolarization. *C*, in the 2~0 concatemer, the hyperpolarization-activated current is sensitive to external pH. The current shown is the tail current at +40 mV after a prepulse to the indicated potential, corrected by the current obtained with a +40-mV prepulse and normalized to the current amplitude under control conditions (−100 mV prepulse, pH 7.5). Data points represent the mean ± S.E. of 5–12 different determinations.

that lead to the bursting behavior normally associated with ClC-0 single-channel currents were not observed in the mixed concatemer.

Even in the absence of a clearly visible common gate, the gating of the pores might be interdependent. We therefore determined the open probability of the large pore in the 1~0 concatemer in relation to the open state of the small pore. The single-channel record was subdivided into sections of small pore open and closed events, and the open probability of the large pore calculated under both conditions. When the small pore was closed, the open probability (at −100 mV) of the large pore was 0.45 ± 0.03 (*n* = 5 patches). When the small pore was open, a value of 0.48 ± 0.02 was obtained, suggesting that the gating of the large pore did not depend on the open state of the small pore. The large pore open probability agrees with the corresponding value for individual pores in homomeric ClC-0, which is ~0.45 at this voltage (10).

Mixed Concatemers of ClC-2 and ClC-0—The gating of ClC-2 differs significantly from ClC-1 and ClC-0. It opens very slowly upon hyperpolarization, is virtually closed at positive potentials, and can be opened by cell swelling and extracellular acidification (24, 25). An N-terminal inactivation domain (residues 21–39) was proposed to influence channel gating from the cytoplasmic side by a ball-and-chain mechanism (24). It is currently unclear how many of these inactivation domains are needed to gate a channel dimer. Possible movement restrictions of the second inactivation domain in the 2~2 concatemer apparently did not interfere with normal gating (compare Fig. 3*A*). However, when we generated mixed concatemers of ClC-2 and ClC-0, only the concatemer with the N-terminal ClC-2 moiety could be expressed functionally. In stark contrast to the ClC-1/ClC-0 concatemers, where the ClC-0 pore dominated the macroscopic current, current traces obtained with the ClC-

2~ClC-0 mixed concatemer showed only a small depolarization-activated ClC-0 type conductance and a rather large hyperpolarization-activated ClC-2 type conductance (Fig. 3*A*).

To investigate whether the hyperpolarization-activated current was indeed carried by ClC-2 pores, we tested its modulation by external pH. The current increased by ~40% upon lowering the pH by 1 unit, and decreased by the same amount upon raising the pH by 1 unit (Fig. 3*C*). This is comparable to the pH sensitivity of ClC-2 wild-type currents, which are increased/decreased by ~60% upon lowering/raising the pH by 1 unit (25). ClC-0 is also weakly dependent on extracellular pH, but the moderate changes of ±1 pH unit employed here would not affect the steady-state current at the test potential of +40 mV (Ref. 17 and results not shown). This demonstrates that pH-dependent activation, which is a characteristic feature of ClC-2, is preserved in the 2~0 mixed concatemer.

Mutational analysis was used to identify the contribution of either pore to the macroscopic current. To this end, point mutations in either of the two subunits were inserted into the 2~0 concatemer and the resulting changes in the macroscopic current analyzed (Fig. 4). The ClC-2(K210Q) mutation accelerated the gating of homomeric ClC-2, resulting in a faster inactivation at depolarized potentials (data not shown). Inserting this mutation in the 2~0 concatemer (Fig. 4, *left panel*) accelerated the decay of the hyperpolarization-activated current upon switching to positive voltages. The K210Q mutation also reduced the hyperpolarization-activated current relative to the current at neutral potentials. This was determined from the ratio of the slope conductances at −120 mV and −40 mV, which was 2.43 and 1.33 for the traces shown in Figs. 3 and 4, respectively. A different effect was seen with the ClC-2(K566E) mutation, which caused outward rectification of the open-pore currents in the homomer (25). This effect is preserved in the
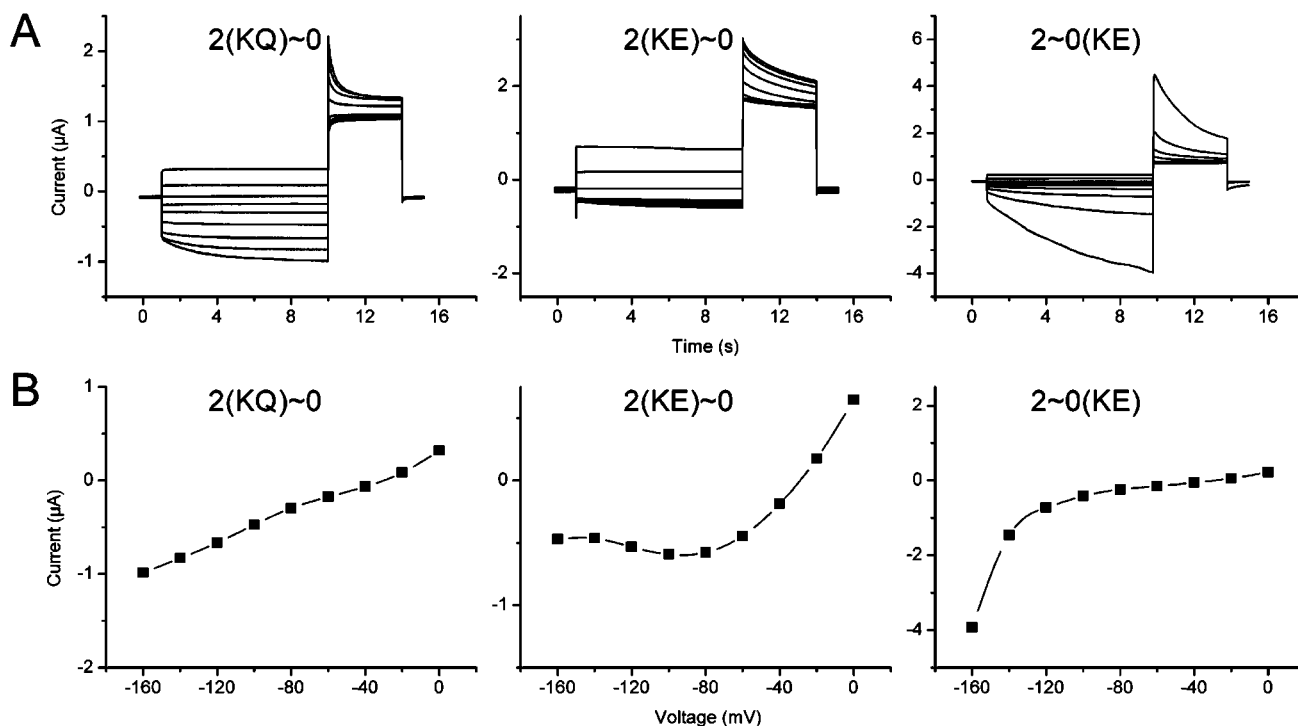
FIG. 4. **Macroscopic properties of mutant ClC-2~ClC-0 concatemers.** *A*, families of current traces obtained with the protocol shown in Fig. 3*A* for three different point mutations in the 2~0 concatemer. *B*, steady-state current-voltage relationships for the traces shown in *A*. The ClC-2(K210Q) mutation accelerates the decay of the hyperpolarization-activated current. The ClC-2(K566E) mutation renders the current outwardly rectifying. Finally, the ClC-0(K519E) mutation greatly reduces the depolarization-activated current, resulting in a conductance resembling that of the ClC-2 homodimer (compare Fig. 3).

mixed concatemer (Fig. 4, *middle panel*), since the current at negative voltages is significantly reduced in comparison with wild-type 2~0 currents. Finally, the ClC-0-like current could be suppressed by the introduction of the ClC-0(K519E) mutation, which greatly reduces the single-channel amplitude (10). The current of the 2~0(K519E) concatemer is only slightly different from that of the 2~2 concatemer (Fig. 4, *right panel*), indicating that a ClC-2 pore with wild-type gating behavior is present in the mixed concatemer.

Single-channel analysis of the 2~0 mixed concatemer is complicated by the fact that no single-channel currents of ClC-2 have been published. Macroscopic currents suggest that the ClC-2 pore should be open only at negative potentials, and noise analysis indicated a single-channel conductance of 2–3 pS (16). When single-channels of the 2~0 concatemer were recorded (Fig. 5), a pore conforming to these predictions was indeed found in association with a ClC-0 type pore. In all recordings that showed a single ~8-pS conductance level, a smaller conductance of 2.8 pS was also found (7 patches). In contrast to the ClC-0 pore, which was always active and gated rapidly, the small pore opened only slowly after switching from positive to negative potential and closed quickly upon returning to positive potential. Once opened by negative voltage, very long open times, interrupted only by brief closings, could be observed (Fig. 5*A*, *bottom trace*).

To finally ascertain the identity of the small pore in the 2~0 concatemer, single-channel recordings of the 2~2 concatemer were performed. This revealed pores with a single-channel conductance of 2.6 ± 0.1 pS (Fig. 6) that gated similarly to the small pore in the 2~0 mixed concatemer. Again, positive voltage caused the pores to close, and upon switching to negative voltage, the pores re-opened only after a significant delay (compare Fig. 6*B*). Unlike the ClC-0, where the slow gating mechanism closes both pores simultaneously, ClC-2 showed no bursting behavior. This constant channel activity of ClC-2, in

combination with its slow activation after a hyperpolarizing voltage step, did not allow us to unequivocally determine the minimum number of active pores, *i.e.* the pore stoichiometry of the homomeric channel.

DISCUSSION

Ever since the first double opening of the *Torpedo* electric organ voltage-gated chloride channel appeared on the chart recorder, the question whether this functional duplicity corresponded also to a structural duplicity, *i.e.* a two-pore channel, has been under debate. For the *Torpedo* channel, ClC-0, it has been answered in favor of two separate conduction pathways in terms of gating behavior (8, 17) and inhibitor blockade (26). The most stringent proof for this "double-barreled" model comes from the analysis of point mutations in mixed concatemers (9, 10, 13). On the other hand, the existence of a common gate that affects both pores simultaneously in ClC-0 (8, 27) and ClC-1 (12), together with dominant negative mutations in ClC-1 that alter channel gating (21) and dominant negative effects of biochemical modification of single monomers in mixed ClC-1 concatemers (11), suggest a functional interaction between both halves of the dimer. The cysteine modification studies of Fahlke and co-workers (11) were even taken as direct evidence for of a single conduction pathway in the dimeric channel, although neither true pore properties nor single-channel behavior were investigated.

The question we have asked is this: are pore properties such as single-channel conductance retained when subunits of different channels are expressed together in a single dimer? If they are, the double-pore arrangement observed in ClC-0 will be extended to other CLC channels. In addition, this will show that the permeation pathway is completely contained in a single subunit of the CLC dimer, as opposed to being lined by parts of either subunit. In mixed concatemers containing ClC-0, we have found that the smallest channel unit consisted

of a single ClC-0 pore accompanied by a smaller pore. The small pore behaved like a ClC-1 pore in the 1~0 concatemer and like a ClC-2 pore in the 2~0 concatemer. Neither pore was encountered alone, but both pores were invariably found together. Moreover, the gating kinetics of the individual pores closely mimic the gating observed in homodimers of the respective subunit. This means that the structures responsible for pore formation and for voltage-dependent (fast) gating are present in any one subunit.

Other properties, however, are dependent on both pores in the dimer. This is clearly the case for the slow gate of the ClC-0, which is no longer seen in the macroscopic current if one ClC-0

FIG. 5. **Single-channel properties of the ClC-2~ClC-0 mixed concatemer.** *A*, current traces of a single channel of the 2~0 concatemer, recorded at −100 mV and −120 mV, are shown. The zero current level is indicated by dashed lines. In addition to the fast-gating ClC-0 pore, a slow-gating smaller pore is also present. At −120 mV, this pore is almost constantly open and shows frequent but very short closings. *B*, the single-pore conductance is determined from the current-voltage relationship in the −80 to −160 mV range. The conductance of the small pore (*triangles*) is 2.8 ± 0.0 pS, and that of the large pore (*squares*) is 8.4 ± 0.2 pS, calculated from a linear fit to the data. Data points represent the mean ± S.E. of two to five individual determinations.

subunit is replaced with a ClC-1 subunit. In the single-channel records of the mixed concatemers, two types of coordinated gating activity may be discerned, the direct transition between fully open and fully closed states, and the direct transition between small and large open levels. The former is nothing else but the slow gating well known in ClC-0, but the latter inter-level transitions would be missed in homomeric channels with two pores of equal conductance. Close inspection of the traces shown (Figs. 2*A* and 5*A*) seems to yield a few examples of either type of gating, *i.e.* coordinated opening/closing events as well as interlevel transitions. Considering the limited bandwidth of our recordings (2 kHz prior to filtering), these could result from incompletely resolved sequential gating events, but we cannot rule out the possibility that coordinated gating activity takes place in the mixed dimers with a low incidence. Since the frequency of these events is in any case too low to significantly alter channel behavior, we have not systematically investigated this example of subunit interdependence.

Furthermore, the contribution of the ClC-1 pore is very much reduced under voltage-clamp conditions when expressed alongside the ClC-0 pore, although both pores are clearly active in excised patches. This discrepancy may be due to the interaction with cytoplasmic cofactors or depend on the low [Cl⁻] of the oocyte interior. Interestingly, in earlier studies of ClC-1 and ClC-2 coexpression (16), ClC-1 contributed little to the macroscopic current (and this most likely resulted from ClC-1 homodimers). Rather, the macroscopic current resembled that of a constitutively open ClC-2 channel. Quite different from the apparent suppression of ClC-1 in the 1~0 and 0~1 concatemers, ClC-2 dominates the macroscopic current in the 2~0 concatemer under whole cell conditions, indicating that ClC-0 is suppressed. Again, in the excised patch, ClC-0 and ClC-2 pores show normal gating.

Assuming that two separate pores are present in a channel consisting of two subunits, the question remains whether one pore is contained completely within a single subunit or formed by parts of each subunit. This question has been addressed in the past in concatemers of ClC-0 carrying two different mutations (10). Although these experiments were fully compatible with a one-subunit/one-pore arrangement, they could not entirely resolve the issue, because the pore structure of CLC channel is not known. The experiments with dimers of two different CLC channels that are reported here demonstrate that the basic channel properties of the monomer are not altered by its interaction with other subunits. This shows that a pore is formed entirely by a single CLC monomer.

We have interpreted our results based on the assumption that only two CLC subunits are required to form a functional channel, but is this justified? Our assumption is well supported by biochemical evidence, which suggests a dimeric structure for ClC-0 (5), ClC-1 (6), and a bacterial CLC homologue (7, 28). Nevertheless, a dimerization of the concatemers used in this
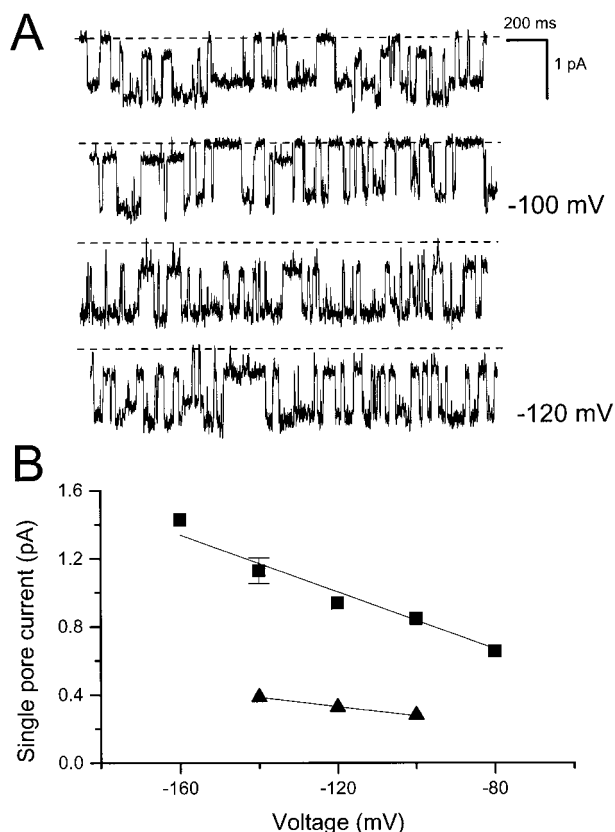
FIG. 6. **Single-channel properties of the ClC-2~ClC-2 concatemer.** *A*, a current trace of a patch most likely containing two channels (four pores), recorded at −120 mV, is shown. The five equidistant current levels are indicated by *dashed lines*. Note the relatively slow gating of the individual pores. *B*, current trace of the same patch, after a switch from 0 mV to −160 mV. Only one pore opens initially, interrupted by brief, flickery closings, until, after a delay of ~10 s, additional pores are activated. The *dashed line* indicates zero current.
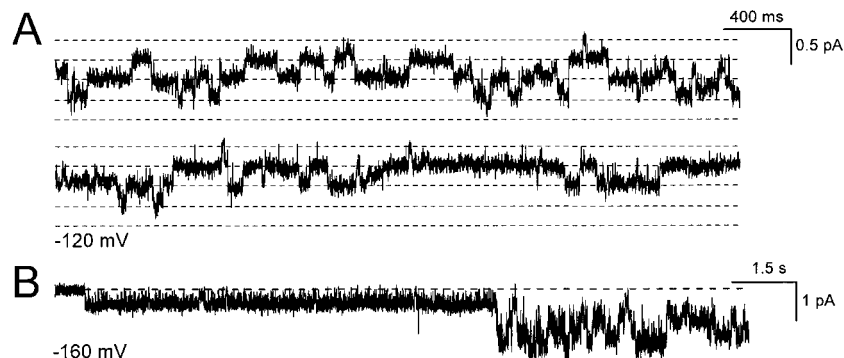
study (resulting in a dimer of dimers) cannot strictly be ruled out. If this should happen, dimers of the two constituent pores rather than mixed dimers could be formed, rendering the single-channel studies meaningless. The presence of single pores of each constituent channel type in the mixed dimers, however, argues against this possibility, for in a tetrameric arrangement, four pores should be present.

Can our results be explained in terms of a single-barreled channel, in which both subunits contribute to a single pore? This alternative model of CLC pore architecture was brought forward by Fahlke *et al.* (11) based on the interaction of single cysteine mutants of ClC-1 with mono- and bifunctional reagents. In the framework of this model, the two equal-sized conductance values observed in single-channel recordings must be regarded as subconductance states of a common pore. A pore consisting of two different CLC proteins, as is the case in our mixed concatemers, could then have two different subconductance states. However, it seems impossible that such subconductance states retain their conductance levels and gating properties they have in the respective homodimer, and that they gate independently of each other in the asymmetric heterodimer.

Taken together, our results argue for a common structural basis of all CLC channels, with a separate conduction pathway, *i.e.* a pore, in each subunit. The fundamental characteristics of channel activity, namely permeation of ions, mirrored in a defined single-channel conductance, and voltage-dependent gating transitions, are present in the monomeric channel and do not depend on the partner subunit. Any CLC dimer, therefore, must be viewed as an association of two basically independent pores. This does not exclude the possibility that some CLC channels are monomers. However, since the dimeric structure found in the bacterial channel (7) appears to be conserved in the mammalian channels, this seems unlikely. Last but not least, we have shown on the single-channel level that ClC-2 is a slowly gating, hyperpolarization-activated channel of 2–3 pS single-channel conductance, in agreement with prior studies of macroscopic currents. This enables a comparison with single-channel recordings from native tissues in which ClC-2 is expressed.

What are the consequences of the one-subunit/one-pore arrangement? One important feature of such a pore architecture is the mechanism by which mutations may affect channel function. In potassium channels, where four subunits contribute equally to a single pore, mutations in the pore as well as in other parts of the protein often have dominant negative effects. On the other hand, mutations in CLC channels will only show a dominant phenotype if they affect a common gating mechanism or if they lead to a retention or misprocessing of hetero-

meric channels before they reach their target membrane. This observation is consistent with the analysis of a dominant negative mutation in ClC-1 causing myotonia congenita (12), which was found to affect the common (slow) gating but not the individual (fast) gating of the channels. Elucidating channel structure may therefore be an important tool for the understanding of mechanisms of pathogenesis in human inherited diseases. The double pore arrangement further implies that the design of dominant-negative mutants, which could be useful in cell biological or transgenic approaches, will not be an easy task for all members of the CLC family.

REFERENCES

1. Akabas, M. H., Cheung, M., and Guinamard, R. (1997) *J. Bioenerg. Biomembr.* **29,** 453–463
2. Sheppard, D. N., and Welsh, M. J. (1999) *Physiol. Rev.* **79,** S23–S45
3. Bormann, J., Rundstrom, N., Betz, H., and Langosch, D. (1993) *EMBO J.* **12,** 3729–3737
4. Jentsch, T. J., Friedrich, T., Schriever, A., and Yamada, H. (1999) *Pflügers Arch.* **437,** 783–795
5. Middleton, R. E., Pheasant, D. J., and Miller, C. (1994) *Biochemistry* **33,** 13189–13198
6. Fahlke, C., Knittle, T., Gurnett, C. A., Campbell, K. P., and George, A. L., Jr. (1997) *J. Gen. Physiol.* **109,** 93–104
7. Maduke, M., Pheasant, D. J., and Miller, C. (1999) *J. Gen. Physiol.* **114,** 713–722
8. Miller, C. (1982) *Philos. Trans. R. Soc. Lond. B Biol. Sci.* **299,** 401–411
9. Middleton, R. E., Pheasant, D. J., and Miller, C. (1996) *Nature* **383,** 337–340
10. Ludewig, U., Pusch, M., and Jentsch, T. J. (1996) *Nature* **383,** 340–343
11. Fahlke, C., Rhodes, T. H., Desai, R. R., and George, A. L., Jr. (1998) *Nature* **394,** 687–690
12. Saviane, C., Conti, F., and Pusch, M. (1999) *J. Gen. Physiol.* **113,** 457–468
13. Ludewig, U., Pusch, M., and Jentsch, T. J. (1997) *Biophys. J.* **73,** 789–797
14. Steinmeyer, K., Ortland, C., and Jentsch, T. J. (1991) *Nature* **354,** 301–304
15. Thiemann, A., Grunder, S., Pusch, M., and Jentsch, T. J. (1992) *Nature* **356,** 57–60
16. Lorenz, C., Pusch, M., and Jentsch, T. J. (1996) *Proc. Natl. Acad. Sci. U. S. A.* **93,** 13362–13366
17. Hanke, W., and Miller, C. (1983) *J. Gen. Physiol.* **82,** 25–45
18. Bauer, C. K., Steinmeyer, K., Schwarz, J. R., and Jentsch, T. J. (1991) *Proc. Natl. Acad. Sci. U. S. A.* **88,** 11052–11056
19. Ludewig, U., Jentsch, T. J., and Pusch, M. (1997) *J. Gen. Physiol.* **110,** 165–171
20. Pusch, M., Ludewig, U., Rehfeldt, A., and Jentsch, T. J. (1995) *Nature* **373,** 527–531
21. Pusch, M., Steinmeyer, K., Koch, M. C., and Jentsch, T. J. (1995) *Neuron* **15,** 1455–1463
22. Astill, D. S., Rychkov, G., Clarke, J. D., Hughes, B. P., Roberts, M. L., and Bretag, A. H. (1996) *Biochim. Biophys. Acta* **1280,** 178–186
23. Rychkov, G. Y., Pusch, M., Astill, D. S., Roberts, M. L., Jentsch, T. J., and Bretag, A. H. (1996) *J. Physiol.* **497,** 423–435
24. Gründer, S., Thiemann, A., Pusch, M., and Jentsch, T. J. (1992) *Nature* **360,** 759–762
25. Jordt, S. E., and Jentsch, T. J. (1997) *EMBO J.* **16,** 1582–1592
26. Miller, C., and White, M. M. (1984) *Proc. Natl. Acad. Sci. U. S. A.* **81,** 2772–2775
27. Lin, Y. W., Lin, C. W., and Chen, T. Y. (1999) *J. Gen. Physiol.* **114,** 1–12
28. Purdy, M. D., and Wiener, M. C. (2000) *FEBS Lett.* **466,** 26–28
29. Pusch, M., Ludewig, U., and Jentsch, T. J. (1997) *J. Gen. Physiol.* **109,** 105–116